Development of 'DFG-out' inhibitors of gatekeeper mutant kinases

Hwan Geun Choi[a,d], **Jianming Zhang**[a,d], **Ellen Weisberg**[b], **James D. Griffin**[b], **Taebo Sim**[a,c,d], and **Nathanael S. Gray**[a,d,*]

[a]Department of Cancer Biology, Dana-Farber Cancer Institute, Boston, MA 02115, USA

[b]Department of Medical Oncology, Dana-Farber Cancer Institute

[c]Life Sciences Research Division Korea Institute of Science and Technology (KIST) 39-1, Hawolgok-dong, Seongbuk-gu, Seoul, 136-791, Korea

[d]Department of Biological Chemistry & Molecular Pharmacology, Harvard Medical School, 250 Longwood Ave, SGM 628, Boston, MA 02115, USA

Abstract

HG-7-85-01(**22**) and HG-7-86-01(**26**) are thiazolo[5,4-b]pyridine containing type II tyrosine kinase inhibitors with potent cellular activity against both wild-type and 'gatekeeper' mutant T315I- Bcr-Abl. Here we report on the 'hybrid design' concept and subsequent structure activity guided optimization efforts that resulted in the development of these inhibitors.

Keywords

T315I Bcr-Abl; Kinase inhibitor; Gatekeeper mutant; Type II inhibitor; Thiazolo[5; 4-b]pyridine

1. Introduction

Despite the tremendous success of the first generation tyrosine kinase inhibitor imatinib for the treatment of chronic myelogenous leukemia (CML), a portion of the patient population eventually develops resistance[1,2]. Three 'second generation' inhibitors: nilotinib,[3] dasatinib[4] and bosutinib,[5] have been approved to treat patients with imatinib resistance however these drugs remain ineffective against T315I 'gatekeeper' mutant form of Bcr-Abl.[6] A 'third generation' of type II inhibitors that effectively inhibit the T315I Bcr-Abl mutant has recently been developed. These inhibitors include AP24163,[7] AP24534,[7] DCC-2036,[8] BGG463,[9] GNF-7,[10] DSA series compounds,[11] and a series of alkynyl inhibitors,[12] of which only AP24534 and DCC-2036 are reported to be undergoing clinical evaluation. Recently, we described the biological characterization of two Type II tyrosine kinase inhibitors: HG-7-85-01(**22**)[13] and HG-7-86-01(**26**)[14] which can potently inhibit the proliferation of cells expressing the major imatinib-resistant gatekeeper mutants T315I-BCR-ABL, T670I-Kit, T674M/I-PDGFRα and T341M/I-Src and which potently and selectively target mutant FLT3. Herein, we describe the hybrid design strategy and

*Corresponding author. nathanael_gray@dfci.harvard.edu (N.S. Gray).

medicinal chemistry effort leading to the development of these ATP-competitive type II inhibitors.

2. Results & Discussion

We have previously reported on the use of a rational "hybrid-design" strategy to convert well known Type I scaffolds into corresponding Type II inhibitors. This approach consists of appending the moiety from a Type II inhibitor that occupies the region adjacent to the ATP-binding site created by the flip of the 'DFG-motif' to the portion of a Type I inhibitor that makes contacts with the hinge region of the kinase.[15] We designed the thiazolopyridine tyrosine kinase inhibitors reported here by hybridizing the hinge interacting thiazole functionality of the Type I inhibitor dasatinib with the 3-trifluoromethylbenzamide pharmacophore present in Type II inhibitors such as imatinib, nilotinib and sorafenib.

The first hybrid compounds that we designed are exemplified by HG-7-85-01 (**22**) and HG-7-86-01 (**26**) and contain a thiazolopyridine core, a 3-trifluoromethylbenzamide Type II 'tail' and various groups appended to the thiazolopyridine (Figure 1). The synthesis of the thiazolo[5,4-b]pyridine core commenced with a Suzuki coupling between commercially available 2-chloro-5-nitropyridine and various phenylboronic acids (Scheme 1). The nitro group was reduced using 5% Pd/C and the resulting product was readily brominated using *N*-bromosuccinimide at low temperature. One-pot 2-(methylthio)thiazole formation was accomplished using potassium ethyl xanthogenate and iodomethane to yield compound **5**. The sulfide group was oxidized with oxone to sulfone compound **6** which could be easily displaced using ammonia in isopropanol. Saponification of ester compound **8** followed by amide coupling using HATU and DIEA provided the target compound **9a**.

The synthesis of compounds **10–13** was accomplished by acylation or amidation of the NH_2 moiety in **9a**. Urea formation to form **14** was accomplished via acylation of **9a** with 4-nitrophenyl chloroformate followed by displacement of the 4-nitrophenyl group with 4-amino-1-Boc-piperidine. The aryl/heteroaryl substituted compounds **15–16** were achieved by palladium catalyzed coupling reactions between **9a** and the appropriate aryl halide and protecting group manipulations.

To evaluate the ability of the compounds to inhibit Bcr-Abl in a cellular context we used the murine pre-B cell line Ba/F3 transformed with the Bcr-Abl oncogene. Wild-type Ba/F3 cells proliferate only in the presence of interleukin-3 (IL-3) while Ba/F3 cells transformed with oncogenic kinases such as Bcr-Abl become capable of growing in the absence of IL-3. This provides a robust and commonly used assay for selective kinase inhibition.[16] The smallest compound **9a** did not display antiproliferative activity against wild-type Bcr-Abl or T315I-Bcr-Abl and the larger compounds **12–16** possessed only weak anti-proliferative activity effect (Table 1). Interestingly, only one compound containing a small cyclopropyl amide displayed submicromolar antiproliferative activity against Bcr-Abl and T315I-Bcr-Abl. Compound **11** exhibited EC_{50}'s of 420 nM on wild-type Bcr-Abl and 960 nM on T315I-Bcr-Abl; however **11** also showed a similar antiproliferative effect against parental Ba/F3 cells suggesting that targets other than Bcr-Abl may contribute to the antiproliferative activity of this compound. To explore this chemical series further we next prepared compounds **20–23** which possess an extended Type II tail containing an (4-ethyl-piperazin-1-yl)methyl moiety appended to the 4-position of the trifluoromethylbenzamide (Table 2). This chemical maneuver resulted in an approximate 6-fold improvement in cellular antiproliferative activity relative to **11** against T315I-Bcr-Abl and a 3-fold decrease in cytotoxicity against parental Ba/F3 cells (Table 2, compound **22**).

We hypothesized that an intramolecular interaction between the thiazole sulfur and the oxygen atom of the adjacent amide in compounds **21–22** contributes to their conformation and biological activity.[17] This is supported by the similar cellular potencies of **21–22** with the 2-pyridine derivative **23**. Compound **23** is predicted to exhibit a similar bioactive conformation to **21–22** as a result of a lone pair of electrons from the pyridine N interacting with the unfilled orbitals of the thiazole sulfur as shown by previous computational analysis.[18] Finally we established the bioactive conformation of this series of compounds by elucidation of a co-crystal structure between HG-7-85-01(**22**) and Src (Figure 2, PDB code: 4AGW). The structure revealed that the distance between the sulfur and oxygen is 2.7 Å which is shorter than the sum of the normal oxygen and sulfur van der Waals radii of 3.3 Å. Consistent with the 'hybrid-design' strategy, compound **22** was confirmed to bind to the DFG-out 'inactive' conformation of Src.[11]

We next further explored substitution on the 3-trifluorophenyl moiety which occupies the pocket created by the 'DFG-out' flip of the activation loop (Table 3, **24–26**). Compound **24**, which eliminates the methylene spacer between the aryl group and piperazine in **22**, lost approximately 10-fold cellular activity relative to **22**. Compound **25** lacking the CF_3 group was completely inactive up to the highest concentration tested (10μM). Compound **26**, which possesses the 'tail' moiety of nilotinib exhibited slightly diminished potency relative to compound **22** but substantially improved the overall kinase selectivity as demonstrated below. We next explored the effects of introducing a flag-methyl or 2-fluoro onto the central phenyl ring (Table 3, **27–30**). The compounds exhibited enhanced activity on Bcr-Abl but not on T315I-Bcr-Abl. For example, compound **27** is an exceptionally potent as inhibitor of wild-type Bcr-Abl dependent Ba/F3 cell proliferation. We also investigated the effect of reversing the amide between the central phenyl and CF_3-substituted ring and replacing the amide with a urea moiety. The synthesis of these compounds is depicted in Scheme 2B. Reversing the amide bond orientation, compound **33** compared to **22**, resulted in approximately a 4-fold reduction in cellular activity against T315I-Bcr-Abl. Interestingly, introduction of a urea linkage (**32**) resulted in 5–10 fold improved activity on both wild-type and T315I Bcr-Abl, but increased cytotoxicity towards parental Ba/F3 cells by approximately 5-fold.

The kinase selectivity of HG-7-85-01(**22**) and HG-7-86-01(**26**) was evaluated using the KINOME*scan*™ approach (Ambit Biosciences, San Diego, CA) against a panel of 353 kinases at a concentration of 10 μM.[19] The kinases which interacted with **22** and **26** with an Ambit score less than 10% of the DMSO control are highlighted with a red circle in a spot tree (Figure 3, supplemental material contains full screening data for **22** and **26**). To provide a measure of overall kinase selectivity we calculated S(10) scores, which is defined as the ratio of the number of kinases inhibited below a score of ten versus total number of kinases tested at a specified concentration. This analysis revealed that compound **26** possess an S(10) of 0.36 and compound **22** possesses an S(10) of 0.10 at a concentration of 10 uM.

We assessed the pharmacological properties of compound **22** and **26** in rats following oral and intravenous delivery (Table 4) prior to performing the murine tumor models which we have previously reported.[13] HG-7-85-01(**22**) has limited oral bioavailability (%F = 18.8), a moderate half-life ($T_{1/2}$ = 5.8 hours), a relatively low maximal serum concentration (C_{max} = 292 ng/mL at 2 mg/kg) and a relatively high clearance (Cl = 13 ml/min/kg). HG-7-86-01(**26**) has poor oral bioavailability (%F = 4.7), however has better exposure as indicated by AUC (111167 min*ng/ml).

In summary, we have used a rational hybrid-design approach to design a new type II scaffold by combining functionality from the type I inhibitor dasatinib with moieties from the type II inhibitors imatinib, nilotinib and sorafenib. The compounds such as **22** and **26** are

capable of potently inhibiting wild-type and T315I-Bcr-Abl activity in biochemical and cellular assays. Further optimization of this scaffold for inhibition of Bcr-Abl and other potential targets identified by the kinase profiling are currently on-going.

Supplementary Material

Refer to Web version on PubMed Central for supplementary material.

Acknowledgments

References

1. Druker BJ, Tamura S, Buchdunger E, Ohno S, Segal GM, Fanning S, Zimmermann J, Lydon NB. Nat Med. 1996; 2(5):561–566. [PubMed: 8616716]

2. Druker BJ, Sawyers CL, Kantarjian H, Resta DJ, Reese SF, Ford JM, Capdeville R, Talpaz M. N Eng J Med. 2001; 344(14):1038–1042.

3. Weisberg E, Manley PW, Breitenstein W, Bruggen J, Cowan-Jacob SW, Ray A, Huntly B, Fabbro D, Fendrich G, Hall-Meyers E, Kung AL, Mestan J, Daley GQ, Callahan L, Catley L, Cavazza C, Azam M, Neuberg D, Wright RD, Gilliland DG, Griffin JD. Cancer Cell. 2005; 7(2):129–41. [PubMed: 15710326]

4. Shah NP, Tran C, Lee FY, Chen P, Norris D, Sawyers CL. Science. 2004; 305(5682):399–401. [PubMed: 15256671]

5. Puttini M, Coluccia AM, Boschelli F, Cleris L, Marchesi E, Donella-Deana A, Ahmed S, Redaelli S, Piazza R, Magistroni V, Andreoni F, Scapozza L, Formelli F, Gambacorti-Passerini C. Cancer Res. 2006; 66(23):11314–22. [PubMed: 17114238]

6. O'Hare T, Walters DK, Deininger MW, Druker BJ. Cancer Cell. 2005; 7(2):117–9. [PubMed: 15710324]

7. O'Hare T, Shakespeare WC, Zhu X, Eide CA, Rivera VM, Wang F, Adrian LT, Zhou T, Huang W-S, Xu Q, Metcalf CA Iii, Tyner JW, Loriaux MM, Corbin AS, Wardwell S, Ning Y, Keats JA, Wang Y, Sundaramoorthi R, Thomas M, Zhou D, Snodgrass J, Commodore L, Sawyer TK, Dalgarno DC, Deininger MWN, Druker BJ, Clackson T. Cancer Cell. 2009; 16(5):401–412. [PubMed: 19878872]

8. Eide CA, Adrian LT, Tyner JW, MacPartlin M, Anderson DJ, Wise SC, Smith BD, Petillo PA, Flynn DL, Deininger MWN, O'Hare T, Druker B. J Cancer Res. 2011; (71):3189–3195.

9. Program of the Fall Meeting 2008. CHIMIA International Journal for Chemistry. 2008; 62(7–8): 547–557.

10. Choi HG, Ren P, Adrian F, Sun F, Lee HS, Wang X, Ding Q, Zhang G, Xie Y, Zhang J, Liu Y, Tuntland T, Warmuth M, Manley PW, Mestan Jr, Gray NS, Sim T. 2010; 53(15):5439–5448.

11. Seeliger MA, Ranjitkar P, Kasap C, Shan Y, Shaw DE, Shah NP, Kuriyan J, Maly DJ. Cancer Res. 2009; 69(6):2384–92. [PubMed: 19276351]

12. Deng X, Lim SM, Zhang J, Gray NS. Bioorg Med Chem Lett. 2010; 20(14):4196–4200. [PubMed: 20541934]

13. Weisberg E, Choi HG, Ray A, Barrett R, Zhang J, Sim T, Zhou W, Seeliger M, Cameron M, Azam M, Fletcher JA, Debiec-Rychter M, Mayeda M, Moreno D, Kung AL, Janne PA, Khosravi-Far R, Melo JV, Manley PW, Adamia S, Wu C, Gray N, Griffin JD. Blood. 2010; 115(21):4206–4216. [PubMed: 20299508]

14. Weisberg E, Choi HG, Barrett R, Zhou W, Zhang J, Ray A, Nelson EA, Jiang J, Moreno D, Stone R, Galinsky I, Fox E, Adamia S, Kung AL, Gray NS, Griffin JD. Mol Cancer Ther. 2010; 9(9): 2468–2477. [PubMed: 20807780]

15. Okram B, Nagle A, Adrian FJ, Lee C, Ren P, Wang X, Sim T, Xie Y, Xia G, Spraggon G, Warmuth M, Liu Y, Gray NS. Chem Biol. 2006; 13(7):779–86. [PubMed: 16873026]

16. Melnick JS, Janes J, Kim S, Chang JY, Sipes DG, Gunderson D, Jarnes L, Matzen JT, Garcia ME, Hood TL, Beigi R, Xia G, Harig RA, Asatryan H, Yan SF, Zhou Y, Gu XJ, Saadat A, Zhou V, King FJ, Shaw CM, Su AI, Downs R, Gray NS, Schultz PG, Warmuth M, Caldwell JS. Proc Natl Acad Sci USA. 2006; 103(9):3153–8. [PubMed: 16492761]

17. Nagao Y, Hirata T, Goto S, Sano S, Kakehi A, Iizuka K, Shiro M. J Am Chem Soc. 1998; 120(13): 3104–3110.

18. Bilodeau MT, Rodman LD, McGaughey GB, Coll KE, Koester TJ, Hoffman WF, Hungate RW, Kendall RL, McFall RC, Rickert KW, Rutledge RZ, Thomas KA. Bioorg Med Chem Lett. 2004; 14(11):2941–2945. [PubMed: 15125964]

19. Davis MI, Hunt JP, Herrgard S, Ciceri P, Wodicka LM, Pallares G, Hocker M, Treiber DK, Zarrinkar PP. Nat Biotechol. 2011; 29(11):1046–1051.
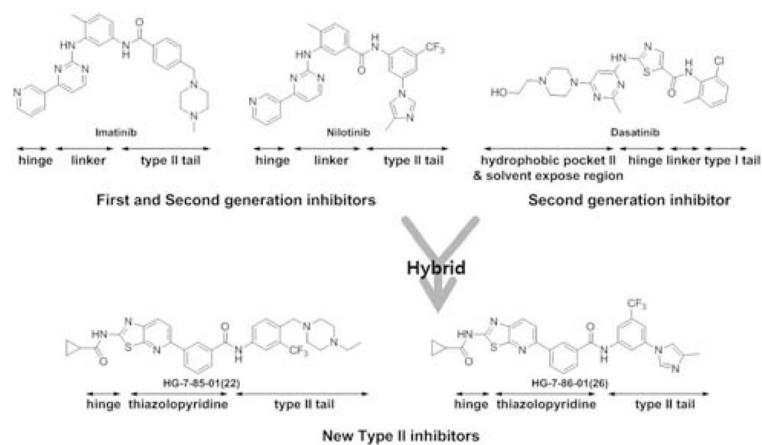
Figure 1.
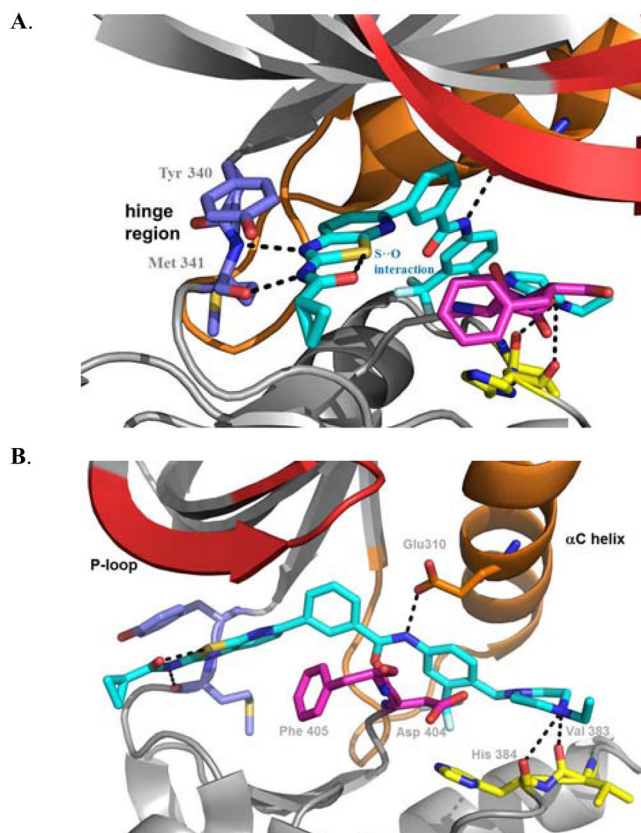Design rational for the thiazolopyridine scaffold

Figure 2.
Compound **22** (turquois sticks) forms five hydrogen-bonding interactions with Src; A. Two hydrogen bonds are made with the hinge region: between the thiazole N and backbone NH of M341 and between the cyclopropyl amide NH and the backbone carbonyl of M341. B. Hydrogen bonding interactions exist between the benzamide carbonyl of 22 and the backbone NH of D404 of the DFG-motif, between the benzamide NH and side-chain carboxylate of E310 from the C-helix, and from the presumably protonated distal piperazine nitrogen and the backbone carbonyls of V383 and H384.
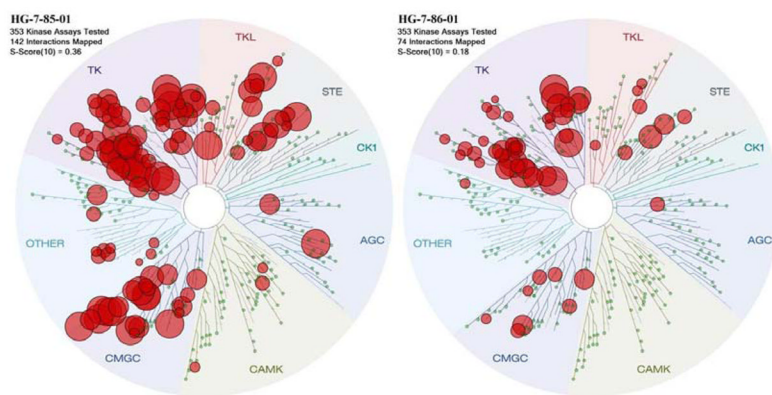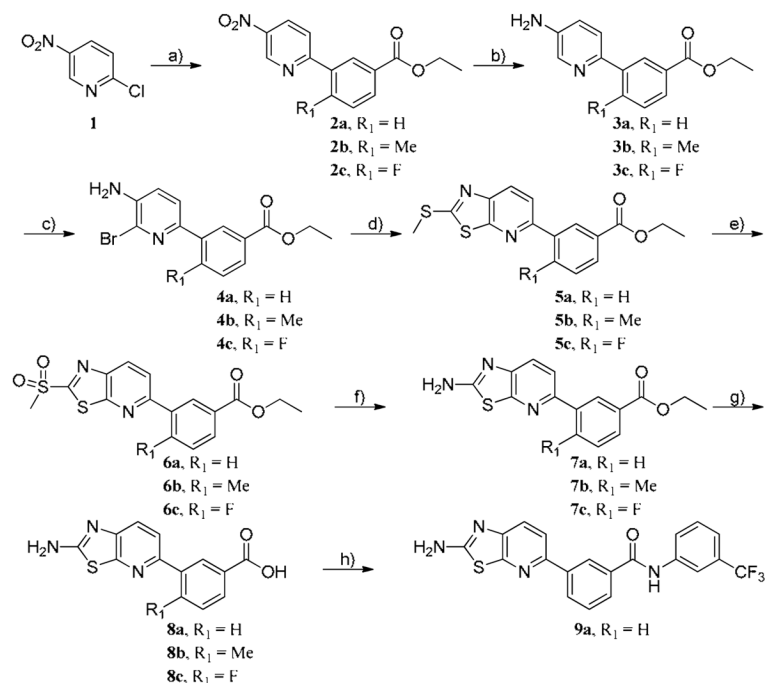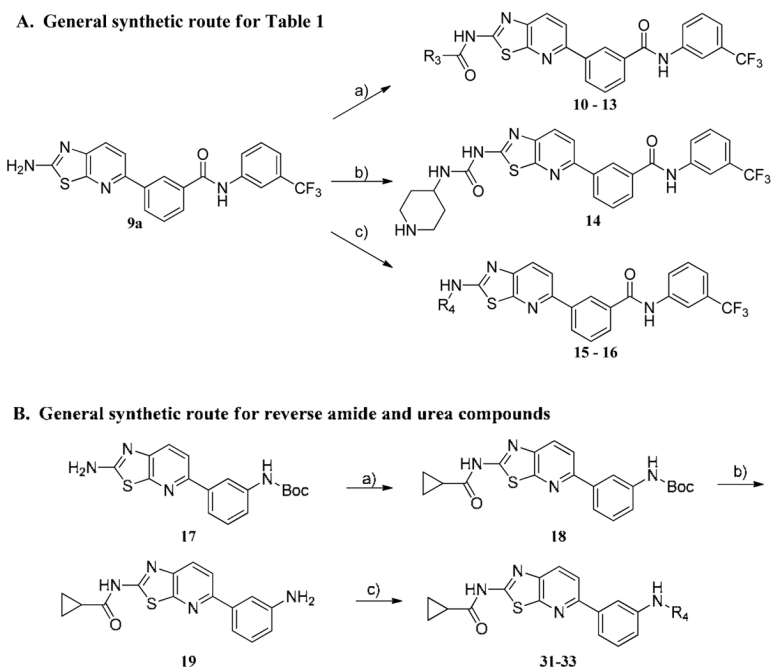
Figure 3.
Kinase Selectivity of HG-7-85-01(22) and HG-7-86-01(26)

**Scheme 1. Reagent and conditions**
a) Boronic acids[(3-(Ethoxycarbonyl)phenylboronic Acid(R_1 = H), 5-Methoxycarbonyl-2-methylphenylboronic acid (R_1 = Me), 5-Ethoxycarbonyl-2-fluorophenylboronic acid (R_1 = F)], Pd(PPh$_3$)$_2$Cl$_2$, *tert*-Butyl XPhos, 2N Na$_2$CO$_3$(aq), dioxane, 90 °C, 10 h, b) 5% Pd/C, EtOH, 16 h, c) NBS, DMF, 0 °C, 5-10 min, d) Potassium ethyl xanthogenate, AcOH, NMP, 150 °C, 16 h and MeI, 50 °C, 30 min, e) Oxone, MeOH, THF, Water, rt, 16 h, f) 2.0 N NH$_3$ in IPA, 90 °C, 24 h, g) LiOH·H$_2$O, THF, MeOH, H$_2$O, rt, 16 h, h) HATU, DIEA, 3-(trifluoromethyl)aniline, DMF, rt, 16 h.
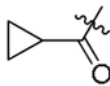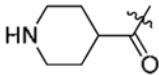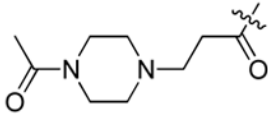
A. General synthetic route for Table 1

B. General synthetic route for reverse amide and urea compounds
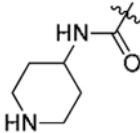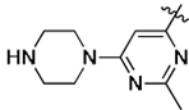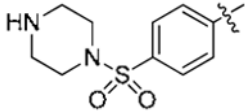

Scheme 2. Reagent and conditions
A. a) Acyl chloride, pyridine, DCM, 0 °C, 4 h or acid, EDCI, HOBT, DMAP, DMF, rt, 8 h, b) i. 4-nitrophenyl chloroformate, pyridine, DCM, rt, 1 h, ii. *tert*-butyl 4-aminopiperidine-1-carboxylate, TEA, THF, rt, 4 h, iii. TFA, DCM, 4 h, c) i. *tert*-butyl 4-(6-chloro-2-methylpyrimidin-4-yl)piperazine-1-carboxylate, Pd$_2$(dba)$_3$, Xanthphos, K$_2$CO$_3$, 2-BuOH, 90 °C, 4 h, ii. TFA, DCM, 4 h. B. a) Cyclopropanecarbonyl chloride, pyridine, DCM, 0 °C, 4 h, b) TFA, DCM, 4 h, c) i. benzoic acid, HATU, DIEA, DMF, 16 h. or *tert*-butyl 4-aminopiperidine-1-carboxylate, TEA, THF, rt, 4h.

Table 1

Cellular antiproliferative activity of compounds **9a-16.**
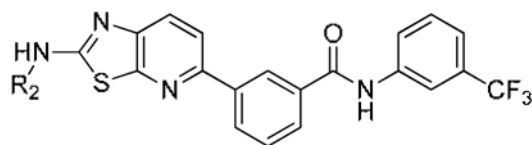
Compds	R_2	Cellular antiproliferative activity (EC$_{50}$, µM)		
		Bcr-Abl (wt)[a]	Bcr-Abl (T315I)[b]	Ba/F3[c]
9a	H	>10	>10	>10
10		5.0	3.77	>10
11		0.42	0.96	0.91
12		>10	>10	>10
13		5.21	>10	>10
14		7.6	7.18	>10
15		1.90	2.41	6.74
16		6.21	>10	>10

[a] Cellular antiproliferative activity (EC$_{50}$, µM) on wt Bcr-Abl-Ba/F3.

[b] Cellular antiproliferative activity (EC$_{50}$, µM) on mutant Bcr-Abl-T315I-Ba/F3.

[c]Cytotoxicity (EC$_{50}$, µM) on wt-Ba/F3.

Table 2

SAR of non-bonded sulfur and oxygen(nitrogen) interaction derivatives.
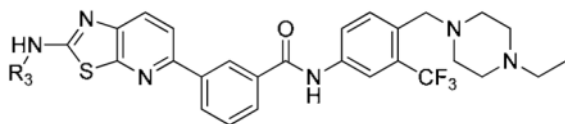
Compds	R₃	Cellular antiproliferative activity (EC$_{50}$, μM)		
		Bcr-Abl (wt)	Bcr-Abl (T315I)	BaF3
20	H	>10	>10	>10
21	acetyl	0.139	0.193	4.16
22	cyclopropanecarbonyl	0.098	0.156	3.085
23	2-pyridinyl	0.146	0.276	3.532

Table 3

Cellular antiproliferation activity of analogs **24–33**.

Compds	Structure	Cellular antiproliferative activity (EC$_{50}$, μM)		
		Bcr-Abl (wt)	Bcr-Abl (T315I)	Ba/F3
24		2.31	2.30	2.30
25		>10	>10	>10
26		0.38	0.19	1.99
27		0.001	0.06	1.23
28		0.03	0.56	4.67
29		0.02	0.30	>10
30		0.02	0.59	>10
31		0.2	0.78	>10
32		0.018	0.013	0.69
33		1.24	0.55	>10

Table 4

Pharmacokinetic results following intravenous 1 mg/kg and oral 2 mg/kg dosing.

Compds	Route of Administration	$t_{1/2}$ (hr)	Tmax	Cmax ng/ml	AUC min*ng/ml	AUC (%extrapolated)	Cl ml/min/kg	MRT (hr)	VSS L/kg	%F
22	PO	4.7	2.7	53.1	27733	35	74.4	7.7		
	IV	5.8	0.08	291.7	73800	35.3	13.7	8.1	6.5	18.8
26	PO	3.7	1.1	32.0	8160	21	303.3	5.3		
	IV	2.4	0.14	671.7	111167	8.7	9.5	3.1	1.7	3.7